Electronic structure, superconductivity, and magnetism in the $C15$ compounds ZrV_2, $ZrFe_2$, and $ZrCo_2$

B. M. Klein, W. E. Pickett, D. A. Papaconstantopoulos, and L. L. Boyer
Naval Research Laboratory, Washington, D.C. 20375
(Received 19 October 1982)

We have calculated the self-consistent paramagnetic electronic structure of cubic Laves-phase ZrV_2, $ZrFe_2$, and $ZrCo_2$, using the augmented-plane-wave method and the local-density-theory form of exchange-correlation potential. Using the mean-field Stoner theory, we have determined the spin susceptibilities and magnetic moments of these compounds. We find that ZrV_2 remains paramagnetic but with large Stoner enhancement, while the system $Zr(Fe_{1-x}Co_x)_2$ is ferromagnetic for $0 \leq x \lesssim 0.5$, in agreement with experiment. However, the Stoner theory yields an average magnetic moment which is generally much too small. The electron-phonon interaction has been calculated and, using estimates of the phononic properties from specific-heat measurements, we compare the theoretical estimates of the superconducting transition temperature with experiment. For ZrV_2, we have found that it is crucial to account for the drop in density of states at the Fermi energy due to the structural phase transition in this material (cubic to rhombohedral at $T_m \sim 100$ K). Estimates of this drop ($\sim 30\%$) have been obtained by analyzing the temperature-dependent spin susceptibility above and below T_m.

I. INTRODUCTION

There has been a great deal of experimental interest in the cubic Laves ($C15$) structure intermetallic compounds due to the wide range of electrical, magnetic, and alloying properties exhibited by many of them. In this paper we present the results of a theoretical investigation of the electronic structure of the $C15$ compounds ZrV_2, $ZrCo_2$, and $ZrFe_2$ using the self-consistent augmented-plane-wave (APW) method. We use these results to study magnetism and superconductivity in these materials

In 1968, Kai *et al.*[1] found that $ZrFe_2$ is a typical ferromagnet, with a Curie temperature of 630 K and a magnetization of 88 emu/g, thought to originate totally from the Fe atoms, with Zr not possessing any moment. This interpretation was consistent with the fact that the separation of Fe atoms in $ZrFe_2$ is nearly identical to that in the metallic state of elemental Fe. On the other hand, $ZrCo_2$ is a Pauli paramagnet,[2] although the pseudobinary system $Zr(Fe_{1-x}Co_x)_2$ is found to become magnetic for $x \lesssim 0.5$[3,4]

The $C15$ compound ZrV_2 is a superconductor with transition temperature $T_c \sim 8$ K.[5-8] It has also been found that this material undergoes a cubic-to-rhombohedral structural phase transition[9] at a temperature $T_m \sim 100$ K. Furthermore, it is known that ZrV_2 has anomalously temperature-dependent properties such as the magnetic susceptibility[8,10] as well as soft-mode behavior[11-14] reminiscent of some of the high-T_c, high—density-of-states $A15$ compounds.[15,16] The pseudobinary system $(Zr_xHf_{1-x})V_2$ shows an interesting correlation between T_c and T_m, viz., the maximum T_c corresponds to the minimum T_m.[8] ZrV_2 is also a good enough hydrogen-storage material to have generated a great deal of technological interest.[17-20] The hydrogen-storage behavior of $ZrCo_2$ on the other hand is quite poor by comparison.[17,21]

The remainder of the paper is organized into six more sections. The APW band-structure methodology used in this work is discussed in Sec. II. In Sec. III we discuss the paramagnetic energy bands and densities of states of these materials, calling attention to various aspects of the bonding that can be determined from the APW calculation. A Stoner model is used to discuss the magnetic properties of the $Zr(Fe_{1-x}Co_x)_2$ pseudobinary system as well as the temperature-dependent Pauli susceptibility of ZrV_2 in Sec. IV. In Sec. V we calculate the electron-phonon interaction in these compounds and, using approximate values for the phononic properties, we estimate the electron-phonon mass-enhancement factor λ as well as T_c. In Sec. VI we give a brief discussion of the electronic specific-heat coefficient γ and in Sec. VII we present our conclusions.

TABLE I. Lattice constants a and MT sphere radii R_A and R_B used in the band-structure calculations for the AB_2 compounds. All values are in atomic units.

	ZrV_2	$ZrFe_2$	$ZrCo_2$
a	14.063	13.360	13.147
R_A	3.045	2.983	2.846
R_B	2.486	2.362	2.324

II. BAND-STRUCTURE METHODOLOGY

The $C15$ (O_h^7 space group) structure Laves-phase compounds we are considering are of the form AB_2 with two formula units per fcc unit cell. By choosing an origin midway between the two A atoms, one obtains real structure factors so that the $C15$ structure may be included in standard APW computer codes,[22] suitably modified to take into account the nonsymmorphic nature of the space group. Maximal nonoverlapping muffin-tin (MT) spheres may be constructed by having the spheres bisect the nearest-neighbor A-A and B-B distances so that $R_A=(\sqrt{3}/8)a$ and $R_B=(\sqrt{2}/8)a$, where a is the *cubic* lattice constant. In this way, 71% of the unit-cell volume may be included in the MT's. Table I gives the values of a, R_A, and R_B used in the present calculations.

Our paramagnetic band-structure calculations follow the symmetrized APW method as discussed by Mattheiss, Wood, and Switendick,[22] modified to include self-consistency and relativistic effects. The latter includes the mass-velocity and Darwin corrections following the method of Koelling and Harmon,[23] and neglects the much smaller (in this case) spin-orbit coupling. No corrections to the standard APW MT approximation were included in these calculations. Owing to the close packing in this structure these corrections are expected to be small. The local-density form of the exchange-correlation potential as given by Hedin and Lundqvist[24] was used in all of our calculations.

The soft-core approximation was used for all of the core states not treated as bands. In this method the core wave functions and resulting charge density are calculated atomiclike in each self-consistent (SC) cycle using the current crystal potential as input into the relativistic Hartree-Fock-Slater atomic structure code of Liberman, Cromer, and Waber (LCW).[25] This code is fully relativistic and includes spin-orbit coupling. The core configurations used were [Ar] for V, Fe and Co, and [Kr] for Zr.

To begin the SC cycles, starting MT charge densities were generated by overlapping atomic spherical charge densities from five neighboring shells of atoms. These densities were obtained using the LCW code with valence configurations $3d^34s^2$, $3d^64s^2$, $3d^74s^2$, and $4d^25s^2$ for V, Fe, Co, and Zr, respectively. From the MT charge densities the starting Coulomb and exchange-correlation potentials were formed using standard techniques.[26]

In the SC procedure, APW eigenvalues and eigenfunctions are calculated for the valence conduction states on a $\vec{k}$-space mesh, states are filled up to the Fermi level by occupying them with the appropriate number of electrons, and an occupied charge density is formed for the MT spheres and the interstitial region. As mentioned above, the core charge density is recalculated in each cycle. To ensure stability we mixed 20% of the new APW charge density with 80% of the charge density from the previous cycle in forming the MT Coulomb and exchange-correlation potentials for the next cycle. Convergence was considered to have been achieved when the eigenvalues from successive cycles were stable to ± 3 mRy or better. For all three compounds con-

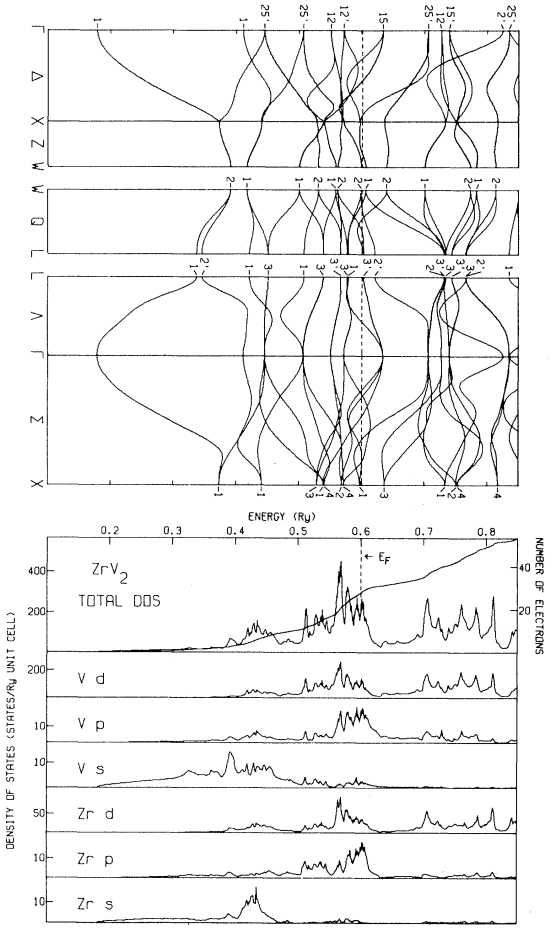

FIG. 1. Energy bands and DOS's for ZrV_2.

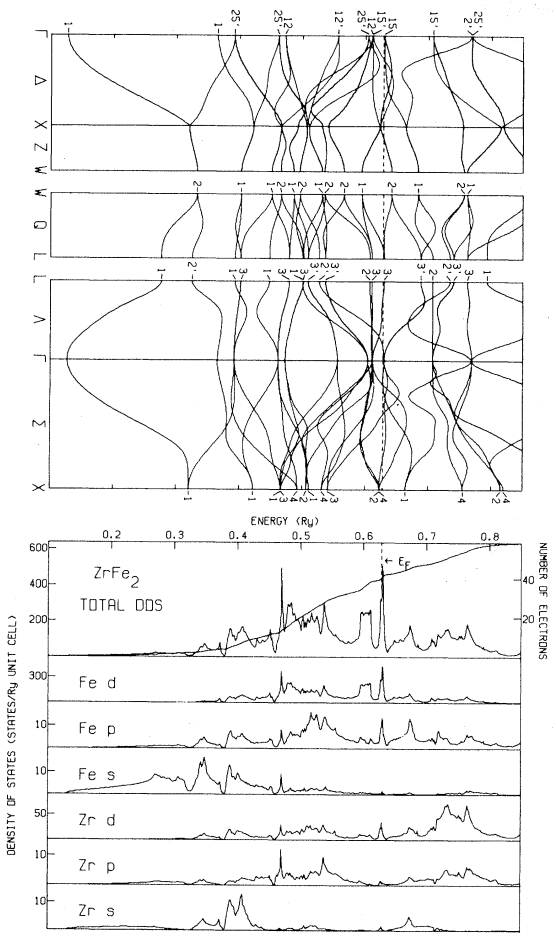

FIG. 2. Energy bands and DOS's for $ZrFe_2$.

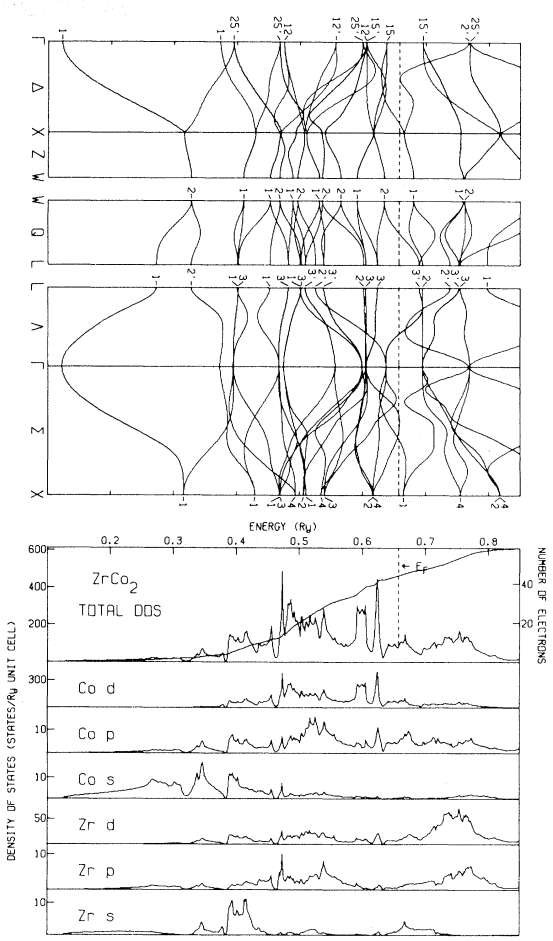

FIG. 3. Energy bands and DOS's for $ZrCo_2$.

sidered here eight SC cycles were needed. A mesh of six $\vec{k}$ points in the irreducible Brillouin zone (IBZ) [32 $\vec{k}$ points in the full Brillouin zone (BZ)] was used in the SC iterations. These were the points $\Gamma(000)$, $\Delta(010)$, $X(020)$, $L(111)$, $W(120)$, and $\Sigma(110)$, all in units of π/a.

After self-consistency was achieved, a final APW run was done on a mesh of 32 $\vec{k}$ points in the IBZ for determining the density of states (DOS). This mesh includes the $\vec{k}$ points on the "standard" 20-$\vec{k}$-point fcc mesh plus 12 additional points, four along the Δ direction, four along the Σ direction, and two along both the Λ and Z directions, respectively. The APW results for 32 $\vec{k}$ points were interpolated onto a mesh of 89 $\vec{k}$ points using Boyer's symmetrized Fourier method[27] and tetrahedral integration[28–30] was used to determine the DOS's.

We finally note that our symmetrized APW's were constructed using

$$|\vec{k}+\vec{G}|^2_{\max}=160(\pi/a)^2 .$$

This yielded eigenvalues converged to 1 or 2 mRy. The dimensions of the symmetrized APW matrices were up to 154 for the twofold-symmetry points on the 20-$\vec{k}$-point mesh. The calculations were performed on a Texas Instruments Advanced Scientific Computer.

III. ENERGY BANDS AND DOS's

Figures 1–3 show the energy bands and DOS's, both total $n(E)$ and site- and angular-momentum-decomposed $n_l^{A(B)}(E)$, of ZrV_2, $ZrFe_2$, and $ZrCo_2$. Table II presents DOS values at E_F together with the SC charges $Q_l^{A(B)}$ in the MT spheres and the rms Fermi velocities $V_F=(\langle V^2\rangle_{E_F})^{1/2}$. Jarlborg and Freeman[31] have published linear muffin-tin orbital (LMTO) band-structure calculations for ZrV_2. Our

TABLE II. Fermi energy E_F (Ry), DOS, both total, n_{tot}, and decomposed by site α and angular momentum l (states/Ry unit cell both spins), MT charges Q_l^α (electrons/atom), charge in the interstitial region Q_{out} (electrons/unit cell), and rms Fermi velocity V_F (10^8 cm/sec), for the AB_2 compounds.

		E_F	n_{tot}	n_s^α	n_p^α	n_d^α	n_f^α	n_{tot}^α	Q_s^α	Q_p^α	Q_d^α	Q_f^α	Q_{in}^α	Q_{out}	V_F
	Zr			0.7403	14.75	29.62	1.022	46.13	0.432	0.495	2.065	0.062	3.054		
ZrV_2		0.6010	222.1											5.74	0.2783
	V			2.219	18.40	111.8	1.057	133.5	0.404	0.321	3.291	0.021	4.037		
	Zr			0.9411	1.487	25.03	0.4799	27.94	0.340	0.381	1.646	0.067	2.434		
$ZrFe_2$		0.6281	321.2											5.34	0.1690
	Fe			0.1551	8.939	265.5	0.8295	275.4	0.455	0.391	6.580	0.022	7.448		
	Zr			1.282	0.7235	7.822	0.3343	10.16	0.328	0.355	1.701	0.068	2.452		
$ZrCo_2$		0.6577	78.99											5.35	0.4932
	Co			0.4979	4.580	57.39	0.1647	62.63	0.466	0.416	7.533	0.022	8.437		

results in Fig. 1 are very similar to theirs.

From Figs. 2 and 3 we note that the energy bands and DOS's of $ZrFe_2$ and $ZrCo_2$ are very similar. For the regions shown, the $E(\vec{k})$ values differ by ~ 10 mRy or less, and the overall DOS structures are in good quantitative agreement for both materials, although there are some differences in the fine structure. Of course the Fermi energy E_F is higher in $ZrCo_2$ due to the extra Co electron (four extra electrons per unit cell), but the DOS's in the region between the different E_F values for the two materials are also very similar. This behavior suggests that the rigid-band model (RBM) is a reasonable approximation for the electronic structure of the $Zr(Fe_{1-x}Co_x)_2$ system. Indeed we find that the RBM is successful in quantitatively explaining the magnetic moment variation in this pseudobinary system (see Sec. IV).

For all three compounds there is a low-lying bonding Zr—B s-like band beginning at 0.179, 0.128, and 0.123 Ry for ZrV_2, $ZrFe_2$, and $ZrCo_2$, respectively. These bandwidths, as measured by the $\Gamma_1 - X_1$ energy difference, are nearly the same for all three compounds (~ 0.2 Ry). From Figs. 1—3 it is seen that in the region ~ 0.4—0.65 Ry the B atom d states are dominant, with important contributions from the Zr d states and others as well. The Fe and Co d states appear to be confined to this energy range, while the V d states are seen to have additional significant contributions in the range of 0.7 Ry and above. The hydridization between the V d states and the V p and the Zr p and d states is strongest in the region around 0.6 Ry, where the Fermi level falls, while the corresponding states in the Fe and Co compounds are more diffuse. In these latter compounds the Zr d states show peaks between 0.7 and 0.8 Ry.

The Fe and Co d states are also more spatially confined than those of V. This can be seen by noting from Table II that the MT charges are $Q_d^{\text{V}} = 3.291$, $Q_d^{\text{Fe}} = 6.580$, and $Q_d^{\text{Co}} = 7.533$, and realizing that Q_d^{Fe} and Q_d^{Co} exceed Q_d^{V} by *more* than the three (four) extra electrons in Fe(Co) compared to V. This is in spite of the fact that the Fe and Co MT radii are smaller than V due to the smaller lattice constants of the former two. We also note that this is not a "charge-transfer" effect, as the Zr SC MT charges for all three compounds are numerically similar when one accounts for the different MT radii. Further evidence for the localized nature of the Fe and Co d electrons follows from noting that over 90% of the charge of the extra d electron in $ZrCo_2$ compared to $ZrFe_2$ is contained in the MT sphere ($Q_d^{\text{Co}} - Q_d^{\text{Fe}} = 0.95$).

A further indication of the bonding in these compounds follows from comparing the SC and starting

MT charges and examining the changes

$$\Delta Q^{A(B)}=\sum_l [Q_l^{A(B)}(\mathrm{SC})-Q_l^{A(B)}(\mathrm{starting})] .$$

We find that $\Delta Q^{\mathrm{Zr}}=-0.37$, -0.50, and -0.52, respectively, for ZrV_2, $ZrFe_2$, and $ZrCo_2$; and $\Delta Q^{\mathrm{V}}=+0.01$, $\Delta Q^{\mathrm{Fe}}=0.09$, and $\Delta Q^{\mathrm{Co}}=0.12$. We see that the B atom charges show small positive changes while the Zr charges decrease considerably. This indicates that the Zr wave functions spread out, or are somewhat depopulated, in the Laves compounds. It should be kept in mind that these interpretations are dependent on the starting atomic configurations used in our calculations.

The Fermi levels in ZrV_2 and $ZrFe_2$ fall in a peak in the DOS and the $n(E_F)$ values are quite large. Recalling that there are six atoms per unit cell, we see from Table II that $n(E_F)=37.0$ and 53.5 states/Ry atom for ZrV_2 and $ZrFe_2$, respectively. Compare these with the value of 25 states/Ry atom typical of the high-T_c $A15$ materials such as V_3Si. From the enormous value of $n(E_F)$ for $ZrFe_2$ we anticipate a prediction of a magnetic instability for this compound (see Sec. IV), in accord with experimental observations.[1] For ZrV_2 we do not find a magnetic instability, but the large value of $n(E_F)$ for the cubic structure, and the rapid variation of $n(E)$ near E_F shown in Fig. 4, would seem to indicate that the cubic-rhombohedral phase transition may be strongly related to an electronically induced instability reminiscent of the $A15$ materials.[15] In particular, we see from Fig. 4 that $n(E)$ varies by $\pm 15\%$ from the value of $n(E_F)$ in a 3-mRy range around E_F. From Fig. 1 it is seen that this peaked structure near E_F corresponds to extremely flat bands near the Fermi energy along the $\Sigma[110]$ direction close to the X point, with some additional flat-band contributions near the W and L points. We note that the peaked $n(E)$ structure near E_F which we obtain appears not to be very sensitive to the limited number of first-principles $\vec{k}$ points that we have used, nor to the interpolation scheme. This conclusion results from comparing these $n(E)$ results with a similarly performed calculation using only 20 $\vec{k}$ points (instead of 32) as input into Boyer's interpolation scheme,[27] and observing that there are only relatively small quantitative changes of a few percent in the DOS results.

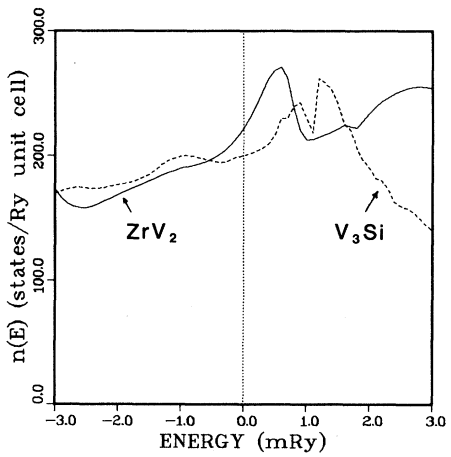

FIG. 4. Total DOS of ZrV_2 (solid curve) and, for comparison, V_3Si (dashed curve) from Ref. 16, near the Fermi energy which is chosen as the zero of energy.

IV. MAGNETIC PROPERTIES

Although all of our energy-band calculations were performed for a paramagnetic system, here we will discuss the magnetic properties for the three compounds based on the Stoner theory of magnetism.[32–36] The procedures that we have used are discussed fully by Vosko and Perdew,[34] Gunnarsson,[35] and Janak.[36]

In the Stoner theory, the exchange-enhanced spin susceptibility at $T=0$ is given by

$$\chi_{\mathrm{sp}}=\mu_B^2 n(E_F)/[1-n(E_F)I_F] , \tag{1}$$

where μ_B is the Bohr magnetron and I_F is a generalized Stoner parameter which can be calculated from the paramagnetic band structure by the following equations[36]:

$$I_F=\int_{\text{unit cell}} d^3r\, \gamma^2(\vec{r})\,|K(\vec{r})| , \tag{2}$$

with

$$K(\vec{r})=\frac{1}{2}\frac{\delta^2 E_{\mathrm{xc}}(\rho,m)}{\delta m(\vec{r})^2}\bigg|_{m=0} , \tag{3}$$

$$\gamma(\vec{r})=\sum_i \frac{\delta(E_F-E_i)\,|\psi_i(\vec{r})|^2}{n(E_F)} , \tag{4}$$

where

$$n(E_F)=\sum_i \delta(E_F-E_i) . \tag{5}$$

Here i denotes a combined wave vector, spin, and band index, $\rho(\vec{r})$ is the charge density, $m(\vec{r})$ the magnetic moment density, and E_{xc} is the local-spin-density exchange-correlation energy functional. It is straightforward to combine the contributions to I_F from the individual MT's and from the interstitial region.

The Stoner theory predicts a magnetic instability when

$$I_F n(E_F)\geq 1 . \tag{6}$$

Furthermore, following the discussion of Gunnarsson,[35] which assumes a rigid spin splitting of the

TABLE III. Total DOS at E_F, $n(E_F)$ (states/Ry unit cell for both spins), generalized Stoner parameter $I_F^{A,B}$ (mRy atom), total Stoner parameter I_F (mRy unit cell), Stoner factor $S=[1-n(E_F)I_F]^{-1}$, and magnetic moment $\bar{m}$ (per unit cell), using the exchange-correlation functional of Ref. 37. The numbers in parentheses under I_F^{total} were calculated using the exchange-correlation functional of Ref. 38 and are shown for comparison.

AB_2	$n(E_F)$	I_F^A	I_F^B	I_F^{total}		$n(E_F)I_F$	S	$\bar{m}$
$ZrFe_2$	321.2	0.056	1.716	6.979	(6.763)	2.242	−0.805	2.17
$ZrCo_2$	79.0	0.126	1.431	5.982	(5.805)	0.473	1.896	0
ZrV_2	222.1	0.303	0.674	3.330	(3.258)	0.740	3.840	0

bands, the magnetic moment may be defined as the solution of the equation

$$\bar{m}=[E(N_+)-E(N_-)]/I_F\ , \tag{7}$$

where, for a total number N of electrons,

$$N_\pm=(N\pm\bar{m})/2\ , \tag{8}$$

with $N_\pm$ being the number of electrons of one spin that are occupied in the ferromagnetic system, and $E(N_\pm)$ are the energies corresponding to occupying $N_\pm$ electrons of one spin which are determined by inverting the values of the energy-integrated $n(E)$. Taking the limit $\bar{m}\to 0$ in Eq. (7) results in the equality in Eq. (6). Our calculated values of I_F, $n(E_F)I_F$, and $\bar{m}$, as well as the Stoner enhancement factor

$$S=[1-n(E_F)I_F]^{-1}\ ,$$

are shown in Table III. The exchange-correlation energy functional of von Barth and Hedin[37] as modified by Janak[36] was used in these calculations. With the use of the recently proposed functional of Vosko, Wilk, and Nusair[38] we obtained results for I_F which differ by approximately 3%. A final general comment is that the interstitial contribution to I_F is negligible, being 1% or less for all three compounds.

A. $ZrFe_2$ and $ZrCo_2$

The magnetic properties of the pseudobinary system $Zr(Fe_{1-x}Co_x)_2$ have been studied by Muraoka *et al.*[3] in most of the composition range $0\le x\le 1$. Here we use the Stoner theory outlined above to determine the magnetic moment $\bar{m}(x)$ in this system. For $x=0.0$ or 1.0 the procedure is well defined; in the intermediate ranges we use the RBM to estimate $n(E,x)$, $I_F(x)$, $E(N_\pm,x)$, and $\rho(r,x)$ needed in the Stoner theory. We used the form

$$\rho(r,x)=(1-x)\rho_{ZrFe_2}(r)+x\rho_{ZrCo_2}(r)\ ,$$

and the values of $n(E,x)$ were determined from the DOS results for $ZrFe_2$.

Our results for $\bar{m}(x)$ are compared with the experiments of Muraoka *et al.*[3] in Fig. 5. We see that the Stoner theory underestimates $\bar{m}(0)$, and generally $\bar{m}(x)$, by more than a factor of 3, although the overall experimental trend is reproduced by the Stoner theory.

One possible reason for the quantitative breakdown of the rigid-band-splitting Stoner theory for transition-metal compounds is the mechanism of "covalent magnetism" recently discussed by Williams *et al.*[39] They argue that in transition-metal compounds there may be spectral-weight shifts from magnetization-induced changes in the interatomic covalent bonding between transition-metal atoms not accounted for in the Stoner theory. Recall that in the Stoner theory the paramagnetic energy bands are assumed to be *uniformly split by the magnetic interaction* in a rigid-band sense, and rearrangements in the shapes of the spin-up or -down $n(E)$ are *not* included. Williams *et al.*[39] give several examples of compounds (e.g., VPd_3) where the Stoner theory accounts for only a small fraction of the total magnetic moment (when compared with results from a spin-polarized energy-band calculation). There is

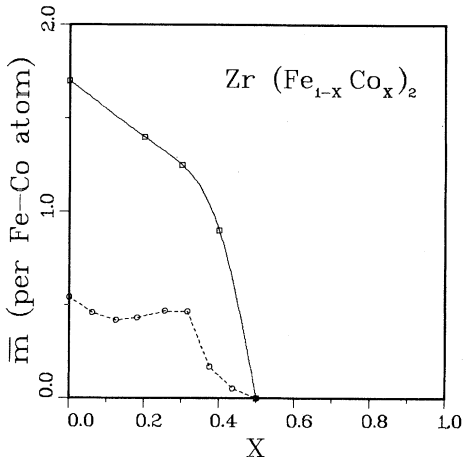

FIG. 5. Experimental (squares) and theoretical (circles) average magnetic moment from Stoner theory in the system $Zr(Fe_{1-x}Co_x)_2$. Solid line connecting the experimental points and the dashed line connecting the theoretical points are guides for the eye.

also the possibility of the existence of local moments in the pseudobinary Fe-Co Laves compounds which are not accounted for in the band (itinerant) magnetism picture. Wiesinger and Hilscher[4] discuss some of these ideas in a recent paper. However, since the Stoner theory fails quantitatively for stoichiometric $ZrFe_2$, a system we believe possesses itinerant magnetism, the discrepancy between theory and experiment probably results from a breakdown of the approximations used in the Stoner theory.

B. ZrV_2

Marchenko and Polovov[8] have measured the magnetic susceptibility of ZrV_2 from approximately 20–300 K in both the cubic ($T \gtrsim 125$ K) and rhombohedral ($T \lesssim 125$ K) phases. They find a significant temperature variation in $\chi(T)$ as well as a sharp drop below the structural phase transition at 125 K. In order to compare our results with theirs we first have to generalize the Stoner theory to finite temperature since the variation in $\chi(T)$ found experimentally may result from the variation in $\chi_{sp}(T)$ induced by the fine structure in $n(E)$ near E_F (see Fig. 4).

Following the development of Pickett,[40] we write

$$\chi(T)=\chi_{orb}+\chi_{sp}(T) , \tag{9}$$

with χ_{orb} an assumed temperature-independent orbital contribution, and

$$\chi_{sp}(T)=\mu_B^2 \frac{n(T)}{1-I_F n(T)} . \tag{10}$$

Comparing Eq. (10) with Eq. (1) we see that the finite-temperature expression involves replacing $n(E_F)$ by the quantity $n(T)$ which is determined from the thermal-occupation expression

$$n(T)=\int_{-\infty}^{+\infty} \left[-\frac{\partial}{\partial E} f_0(E-\zeta(T)) \right] n_{eff}(E)dE , \tag{11}$$

where f_0 is a Fermi function and $\zeta(T)$ is the chemical potential determined from conservation of electrons. The quantity $n_{eff}(E)$ is an effective density of electronic states which for strongly interacting electron-phonon systems accounts for the effects of thermal lattice disorder by the expression

$$n_{eff}(E)=\int_{-\infty}^{+\infty} dE' n(E') \frac{\Gamma/\pi}{(E-E')^2+\Gamma^2} . \tag{12}$$

We use the broadening halfwidth given by

$$\Gamma \approx \pi \lambda_{tr} k_B T , \tag{13}$$

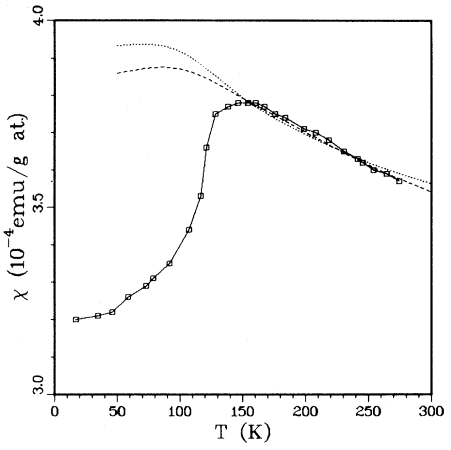

FIG. 6. Experimental (Ref. 8) susceptibility $\chi(T)$ of ZrV_2 (connected squares) compared with theoretical calculations using Eqs. (9)–(13). Theoretical results are for assumed values of λ of 1.0 (dashed curve) and 2.0 (dotted curve). (See discussion in Sec. IV.)

which is the asymptotic form valid for $T \gg \Theta_D$, where Θ_D is the Debye temperature, but holds reasonably well for $T > \Theta_D/2$. Although λ_{tr} is in principle the transport equivalent of the electron-phonon mass-enhancement parameter λ which enters into the superconducting T_c and the electronic specific heat, experience has shown that $\lambda_{tr} \approx \lambda$ to a good approximation.[41]

We compare our theoretical results for $\chi(T)$ with the experimental results of Marchenko and Polovov[8] in Fig. 6. Two calculations of $\chi(T)$ are shown, using $\lambda=1.0$ and 2.0 (the actual value of λ is expected to fall between these two extremes). The corresponding *fitted* values of χ_{orb} are 1.80 and 2.02 emu/g-at., respectively. These values of χ_{orb} are close to the estimates one would get from appropriately weighting the experimental or theoretical values for atomic V and Zr.[42]

From Fig. 6 it is seen that the temperature dependence of $\chi(T)$ above 100 K is well described by either theoretical calculation. In this temperature range ZrV_2 is in the cubic Laves phase corresponding to the crystal structure assumed in the APW calculations. In the region below 150 K, $\chi(T)$ falls precipitously as the crystal undergoes a phase transition to the rhombohedral structure, and our theory, which predicts the cubic state behavior, deviates from the experimental results. Assuming that χ_{orb} does not change due to the transformation, and furthermore neglecting a possible change in I_F, we can estimate the decrease in $n(E_F)$ in the low-temperature phase by comparing

$$[\chi(T \to 0)-\chi_{orb}]_{expt}$$

with

$$\chi_{sp}(T\to 0)=\mu_B^2 n(E_F)/[1-I_F n(E_F)]$$

from the calculations in the cubic phase. We find the ratio

$$\frac{n(E_F)_{\text{rhomb}}}{n(E_F)_{\text{cubic}}}$$

to be 0.73 and 0.67 for $\lambda=1.0$ and 2.0, respectively.

Thus, the susceptibility analysis leads us to conclude that there is a substantial ($\sim 30\%$) reduction in $n(E_F)$ for the transformed crystal. This result is in concert with what one would expect based on the idea that the cubic-to-rhombohedral transition is driven by an instability induced by the high sharp peak in $n(E)$ near E_F which drives a phonon instability. Upon making the phase transition one would expect that the lower-symmetry phase has a reduced $n(E_F)$ value which passivates the phonon instability and therefore leads to an overall stiffening of the phonon spectrum. This has been observed[8] in ZrV_2 and similarly behaving HfV_2 (see below).[43]

V. SUPERCONDUCTIVITY

We have calculated the electron-ion interaction constant η for all three materials using the rigid MT theory of Gaspari and Gyorffy[44]:

$$\eta_\alpha = n(E_F)\langle I^2\rangle_\alpha = \frac{E_F}{\pi^2 n(E_F)} \times \sum_l 2(l+1)\sin^2(\delta_{l+1}^\alpha-\delta_l^\alpha)\frac{n_l^\alpha n_{l+1}^\alpha}{n_l^{(1)\alpha} n_{l+1}^{(1)\alpha}} , \tag{14}$$

where δ_l^α are scattering phase shifts at E_F for atom α and angular momentum l, $n_l^{(1)\alpha}(E_F)$ are "free-scatterer" DOS's defined in Ref. 44, and $n_l^\alpha(E_F)$ are the site-angular—momentum Fermi-level DOS's [the DOS quantities to be used in Eq. (14) are the values per spin, one-half of the numbers given in Table II]. The results are given in Table IV. For ZrV_2, two sets of results of $\eta=\eta_A+\eta_B$ are given, one set using the $n(E_F)$ and $n_l^\alpha(E_F)$ values appropriate to the high-temperature cubic phase, and the other set using values scaled by the factor 0.7, corresponding to our estimate of the reductions in the $n(E_F)$ and $n_l^\alpha(E_F)$ values in the low-temperature rhombohedral phase discussed in the preceding section. This scaled value of η_{rhomb} has been determined with the assumption that the other factors, i.e., phase shifts and $n_l^{(1)\alpha}$, are approximately unchanged so that η scales as $n(E_F)$.

We note that in ZrV_2, $\eta_{Zr}\approx\frac{1}{3}\eta_V$, while Zr makes a much smaller contribution to the total η in $ZrCo_2$ and $ZrFe_2$. Our value for η in the cubic phase of ZrV_2 is 25% smaller than that of Jarlborg and Freeman[31] who used an overlapping MT sphere implementation of the Gaspari-Gyorffy theory.

In order to proceed further and calculate λ and T_c we need estimates of the phonon moments for these materials. Since there are no neutron scattering results available, we use approximate values obtained from specific-heat measurements. In the case of ZrV_2 we can make use of the work of Marchenko and Polovov[8] in determining the geometric mean phonon frequency ω_g from an analysis of their experimental specific-heat and susceptibility data. It has been shown previously that ω_g is closely related to the value of the ω_2 phonon moment which enters into the determination of λ,[45,46]

$$\omega_g^2\approx\omega_2^2=\langle\omega\rangle/\langle\omega^{-1}\rangle , \tag{15}$$

so that we make the approximation

$$\lambda\cong\frac{\eta}{\bar{M}\,\omega_g^2} . \tag{16}$$

Here $\bar{M}$ is the average mass in the unit cell, and to estimate the theoretical values of T_c we use the

TABLE IV. Total DOS $n(E_F)$ (states/Ry unit cell both spins), electron-phonon parameters η (eV/Å^2) and λ, phonon moments ω_2 (K) (see text), and calculated and experimental values of T_c (K). For ZrV_2, values for the cubic and rhombohedral phases are given (see text).

AB_2	$n(E_F)$	η_A	η_B	η_{tot}	ω_2	λ	T_c^{calc}	T_c^{expt}
ZrV_2								
Cubic	222.1	2.07	5.79	7.86	225	1.36	17	~ 9
Rhombohedral	155.5	1.45	4.05	5.50	204	1.16	12	~ 8
$ZrCo_2$	79.0	0.34	1.49	1.83	283	0.18	~ 0	0
$ZrFe_2$	321.2	0.34	6.76	7.10	283	0.70	~ 9[a]	0

[a]This theoretical estimate is based on treating $ZrFe_2$ as a paramagnetic material. In actuality, ferromagnetism quenches superconductivity in this compound.

Allen-Dynes[46] modification of the McMillan equation,

$$T_c = \frac{\omega_{\log}}{1.2} \exp\left[-\frac{1.04(1+\lambda)}{\lambda - \mu^*(1+0.62\lambda)} \right], \qquad (17)$$

with $\mu^* = 0.13$ and $\omega_{\log} \cong 0.8\omega_2 \approx 0.8\omega_g$, as is typical for most transition-metal systems.

From Table IV we see that for transforming ZrV_2 the resulting calculated values of λ and T_c are 1.16 and 12 K, respectively. The calculated result for T_c is in reasonable agreement with the experimental value of ~ 8 K, especially considering the approximations that were used in obtaining the theoretical estimate.

Marchenko and Polovov[8] have found that as-cast samples of ZrV_2 do not transform to the rhombohedral phase as the annealed samples do. The nontransforming samples have T_c values slightly higher than those that do transform (about a 1-K increase in T_c). The nontransforming samples also have ω_g values some 10% larger indicating a significantly stiffer phonon spectrum. Performing a calculation for the nontransforming sample using our unscaled (cubic) value of η and a 10% increase in ω_g, leads to values of λ and T_c of 1.37 and 17 K, respectively. The increases in both quantities are qualitatively correct, but too large in magnitude.

We mention two factors which can lower T_c from these calculated values. First, it is clear that the effective electron-phonon interaction λ_{eff} in systems with sharp structure in $n(E)$ which determines T_c is proportional *not* to $n(E_F)$, but to some effective value[40] resulting from virtual phonon exchange averaging $n(E)$ over a range $E_F \pm \omega_{\max}$ with the maximum phonon energy $\omega_{\max} \sim 2$ mRy for ZrV_2. Second, actual ZrV_2 samples contain defects which also broaden structure in $n(E)$. For the DOS function shown in Fig. 4, both of these effects will lower T_c. Also, it appears that only unannealed samples (with large disorder) remain cubic below ~ 125 K, and the large amount of disorder in such samples can account for $T_c \sim 9$ K found experimentally being much lower than the perfect-crystal value which we calculate. Such behavior also occurs in Nb_3Sn and V_3Si.

For $ZrCo_2$ and $ZrFe_2$ there is no information available on the phonon spectra or ω_g, so that the results in Table IV make use of the Debye approximation $\omega_g^2 \approx \frac{1}{2}\Theta_D^2$ in Eq. (16). We find that λ for paramagnetic $ZrFe_2$ is substantial. Of course, the occurrence of ferromagnetism in this material effectively eliminates superconductivity.

VI. SPECIFIC HEAT

Low-temperature specific-heat measurements on ZrV_2 have been reported by Marchenko and Polovov[8] and by Rapp and Vieland.[47] The former measurement gave a value of the electronic specific heat γ of 10.0 mJ/g-at. K^2, while the latter measurement, which was performed in a magnetic field of 105 kG, yielded a value of 16.5 mJ/g-at. K^2. The large differences between the two measurements could result from deviations from stoichiometry, as both sets of experimental results were on samples with some second-phase material. Our theoretical results for $\gamma \propto n(E_F)(1+\lambda)$ are 9.7—14.7 mJ/g-at. K^2, which approximately span the values from the experiments. The theoretical range is due to our estimates for the values of $n(E_F)$ and λ for transforming (rhombohedral, low-γ) and nontransforming (cubic, high-γ) samples. Again, disorder in the nontransforming samples would decrease the perfect-crystal cubic value.

Although specific-heat measurements of $ZrCo_2$ and $ZrFe_2$ are available,[48] the presence of magnetic clusters and ferromagnetism, respectively, have limited the reliability of these measurements for determining γ. Results of different workers differ considerably. Our predictions for good quality $ZrCo_2$ samples (and for ficticious paramagnetic $ZrFe_2$) can be obtained from the data in Table IV.

VII. CONCLUSIONS

We have performed APW band-structure calculations of the paramagnetic electronic structure of the cubic Laves ($C15$) phase compounds ZrV_2, $ZrFe_2$, and $ZrCo_2$, and the results have been applied to calculate and discuss the bonding and several of the variables relevant to magnetism and superconductivity in these materials.

To study the magnetic properties we have used the Stoner theory, finding that ZrV_2 and $ZrCo_2$ are paramagnetic while $ZrFe_2$ is ferromagnetic, in agreement with experiment. However, the calculated magnetic moment of the latter compound is too small by nearly a factor of 3. The magnetic moment of the pseudobinary system $Zr(Fe_{1-x}Co_x)_2$ was also studied using the Stoner theory together with a RBM for $n(E)$, and we have found results in good qualitative agreement with experiment as to the monotonic decrease of the moment with x and the vanishing of ferromagnetism for $x \approx 0.5$, although the calculated moment is too small in the range $0.0 \leq x \leq 0.5$. This result is consistent with the observation by others[39] that the Stoner theory is quantitatively inaccurate in compound systems where

there is significant covalent bonding.

Theoretical estimates for the superconducting parameters η, λ, and T_c have been determined and, in agreement with experiment, we find that $ZrCo_2$ is not a superconductor, ZrV_2 is a relatively high-T_c material, and $ZrFe_2$ has its superconductivity quenched by ferromagnetism. By analyzing the susceptibility data, we have also shown that the structural instability (cubic to rhombohedral at $T_m \sim 100$ K) in ZrV_2 results in a significant lowering of $n(E_F)$ and T_c from the values that would have been obtained if this material remained cubic at low temperatures. In this regard, it is to be noted that there is fine structure in and large values for $n(E)$ near E_F for ZrV_2 on the same scale as has been found in high-T_c $A15$ materials such as V_3Si and Nb_3Sn. The structural instabilities in ZrV_2 are likely to be related to this $n(E)$ behavior as they are for the $A15$'s, although the structural transition temperature in ZrV_2 is somewhat higher.

Further theoretical studies on these materials would seem to be warranted. These should include spin-polarized band-structure calculations for $ZrFe_2$ as well as further research into the origins of the structural instabilities in ZrV_2. Two of us have already used the present band-structure results to study the hydrogen-storage behavior in these materials.[21]

[1]K. Kai, T. Nakamichi, and N. Yamamoto, J. Phys. Soc. Jpn 25, 1192 (1968).

[2]Y. Aoki, T. Nakamichi, and M. Yamamoto, Phys. Status Solidi B 53, K137 (1972).

[3]Y. Muraoka, M. Shiga, and Y. Nakamura, J. Phys. F 9, 1889 (1979), and references therein.

[4]G. Wiesinger and G. Hilscher, J. Phys. F 12, 497 (1982), and references therein.

[5]B. T. Matthias, V. B. Compton, and E. Corenzwit, J. Phys. Chem. Solids 19, 130 (1961).

[6]An extensive bibliography may be found in S. V. Vonsovsky, Yu. A. Izymov, and E. Z. Kurmaev, in *Superconductivity of Transition Metals, Their Alloys and Compounds,* Vol. 27 of *Springer Series in Solid State Sciences* edited by M. Cardona, P. Fulde, and H.-J. Queisser (Springer, Berlin, 1982).

[7]K. Inoue and K. Tachikawa, J. Jpn. Inst. Metals 39, 1266 (1975).

[8]V. A. Marchenkov and V. M. Polovov, Zh. Eksp. Teor. Fiz. 78, 1062 (1980) [Sov. Phys.—JETP 51, 535 (1980)].

[9]D. E. Moncton, Solid State Commun. 13, 1779 (1973).

[10]V. M. Pan, I. E. Bulakh, A. L. Kasatkina, and A. D. Shevckenko, Fiz. Tverd. Tela (Leningrad) 20, 2487 (1978) [Sov. Phys.—Solid State 20, 1437 (1978)]; J. Less-Common Metals 62, 157 (1978).

[11]A. C. Lawson, Phys. Lett. 38A, 379 (1972).

[12]V. A. Finkel' and E. A. Pushkarev, Zh. Eksp. Teor. Fiz. 73, 2332 (1977) [Sov. Phys.—JETP 46, 1220 (1977)].

[13]E. S. Karpov, I. I. Papirov, E. A. Pushkarev, and V. A. Finkel', Fiz. Tverd. Tela (Leningrad) 21, 3551 (1979) [Sov. Phys.—Solid State 21, 2050 (1979)].

[14]M. Levinson, C. Zahradnik, R. Bergh, M. L. A. MacVicar, and J. Bostock, Phys. Rev. Lett. 41, 899 (1978).

[15]See e.g., L. R. Testardi, in *Physical Acoustics,* edited by W. P. Mason and R. N. Thurston (Academic, New York, 1973), Vol. X, p. 193; Yu. A. Izyumov and E. Z. Kurmaev, Usp. Fiz. Nauk 113, 193 (1974) [Sov. Phys.—Usp. 19, 26 (1976)].

[16]See, e.g., B. M. Klein, L. L. Boyer, D. A. Papaconstantopoulos, and L. F. Mattheiss, Phys. Rev. B 18, 6411 (1978); B. M. Klein, L. L. Boyer, and D. A. Papaconstantopoulos, Phys. Rev. Lett. 42, 530 (1979).

[17]M. Peretz, D. Zamir, D. Shaltiel, and J. Shinar, Z. Phys. Chem. Neue Folge 117, S221 (1979).

[18]J. J. Didisheim, K. Yuon, D. Shaltiel, P. Fischer, P. Bujard, and E. Walker, Solid State Commun. 32, 1087 (1979).

[19]I. Jacob, D. Shaltiel, D. Davidov, and I. Miloslavski, Solid State Commun. 23, 669 (1977).

[20]D. Fruchart, A. Rouault, C. B. Shoemaker, and D. P. Shoemaker, J. Less-Common Metals 73, 363 (1980).

[21]B. M. Klein and W. E. Pickett, J. Less-Common Metals 88, 231 (1982). This theoretical work makes use of the present electronic structure results in a study of the hydrogen-storage behavior of ZrV_2 and $ZrCo_2$.

[22]See, e.g., L. F. Mattheiss, J. H. Wood, and A. C. Switendick, in *Methods in Computational Physics,* edited by B. Alder, S. Fernbach, and M. Rotenberg (Academic, New York, 1968), Vol. 8.

[23]D. D. Koelling and B. N. Harmon, J. Phys. C 10, 3107 (1977).

[24]L. Hedin and B. I. Lundqvist, J. Phys. C 4, 2064 (1971).

[25]D. A. Liberman, D. T. Cromer, and J. T. Waber, Comput. Phys. Commun. 2, 107 (1971).

[26]D. A. Papaconstantopoulos and W. R. Slaughter, Computer Phys. Commun. 7, 207 (1974); 13, 225 (1977).

[27]L. L. Boyer, Phys. Rev. B 19, 2824 (1979).

[28]G. Lehmann, P. Rennert, M. Taut, and H. Wonn, Phys. Status Solidi 37, K27 (1970).

[29]G. Lehmann and M. Taut, Phys. Status Solidi 54, 469 (1972).

[30]O. Jepsen and O. K. Andersen, Solid State Commun. 9, 1763 (1971).

[31]T. Jarlborg and A. J. Freeman, Phys. Rev. B 22, 2332 (1980).

[32]E. C. Stoner, Proc. R. Soc. London Ser. A 154, 656 (1936); *ibid.* 169, 339 (1939).

[33]C. Herring, *Magnetism IV,* edited by G. T. Rado and H. Suhl (Academic, New York, 1966), p. 256.
[34]S. H. Vosko and J. P. Perdew, Can. J. Phys. 53, 1385 (1975).
[35]O. Gunnarsson, J. Phys. F 6, 587 (1976).
[36]J. F. Janak, Phys. Rev. B 16, 255 (1977).
[37]U. von Barth and L. Hedin, J. Phys. C 5, 1629 (1972).
[38]S. H. Vosko, L. Wilk, and M. Nusair, Can. J. Phys. 58, 1200 (1980).
[39]A. R. Williams, R. Zeller, V. L. Moruzzi, and C. D. Gelatt, Jr., J. Appl. Phys. 52, 2067 (1981).
[40]W. E. Pickett, Physica 107B, 703 (1981); Phys. Rev. Lett. 48, 1548 (1982); Phys. Rev. B 26, 1186 (1982).
[41]See, e.g., F. J. Pinski, P. B. Allen, and W. H. Butler, Phys. Rev. B 23, 5080 (1981), and references therein.
[42]E. V. Galoshina, Usp. Fiz. Nauk 113, 105 (1974) [Sov. Phys. Usp. 17, 345 (1974)].
[43]J. W. Hafstrom, G. S. Knapp, and A. T. Aldred, Phys. Rev. B 17, 2892 (1978).
[44]G. D. Gaspari and B. L. Gyorffy, Phys. Rev. Lett. 28, 801 (1972).
[45]G. S. Knapp, S. D. Bader, and Z. Fisk, Phys. Rev. B 13, 3783 (1976).
[46]P. B. Allen and R. C. Dynes, Phys. Rev. B 12, 905 (1975).
[47]Ö. Rapp and L. J. Vieland, Phys. Lett. 36A, 369 (1971).
[48]G. Hilscher and E. Gmelin, J. Phy. (Paris) 39, C6-774 (1978).